AD-A138 868 POWER TRANSFER FOR MICROWAVE DISCHARGES(U) SRI INTERNATIONAL MENLO PARK CA G AUGUST ET AL. 23 DEC 83 N00019-82-C-0287 1/1

UNCLASSIFIED F/G 20/9 NL

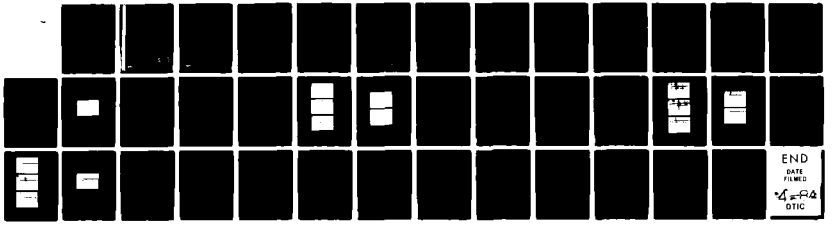

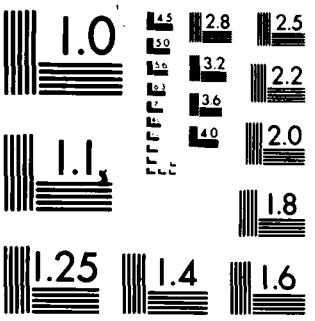

Final Report *December 1983*

POWER TRANSFER FOR MICROWAVE DISCHARGES

By: G. AUGUST S. DAMRON

Prepared for:

NAVAL AIR SYSTEMS COMMAND
DEPARTMENT OF THE NAVY
WASHINGTON, D.C. 20361
Attention: JAMES W. WILLIS, CODE AIR-33

CONTRACT N00019-82-C-0287

SRI Project 4885

SRI International
333 Ravenswood Avenue
Menlo Park, California 94025
(415) 326-6200
Cable: SRI INTL MPK
TWX: 910-373-2046

SRI International

Final Report *December 1983*

POWER TRANSFER FOR MICROWAVE DISCHARGES

By: G. AUGUST S. DAMRON

Prepared for:

NAVAL AIR SYSTEMS COMMAND
DEPARTMENT OF THE NAVY
WASHINGTON, D.C. 20361
Attention: JAMES W. WILLIS, CODE AIR-33

CONTRACT N00019-82-C-0287

SRI Project 4885

Approved by:

JOHN B. CHOWN, *Director*
Electromagnetic Sciences Laboratory

DAVID A. JOHNSON, *Vice President*
System Technology Division

SRI INTERNATIONAL, 333 Ravenswood Avenue, Menlo Park, California 94025
(415) 326-6200, Cable: SRI INTL MPK, TWX: 910-373-2046

SRI International®

UNCLASSIFIED

SECURITY CLASSIFICATION OF THIS PAGE (When Data Entered)

REPORT DOCUMENTATION PAGE	READ INSTRUCTIONS BEFORE COMPLETING FORM
1. REPORT NUMBER	2. GOVT ACCESSION NO. AD-A138 868 / 3. RECIPIENT'S CATALOG NUMBER
4. TITLE (and Subtitle) Power Transfer for Microwave Discharges	5. TYPE OF REPORT & PERIOD COVERED Final Report 20 Sept 1982 to 31 Dec 1983
	6. PERFORMING ORG. REPORT NUMBER SRI Project 4885
7. AUTHOR(s) C. August and S. Damron	8. CONTRACT OR GRANT NUMBER(s) N00019-82-C-0287
9. PERFORMING ORGANIZATION NAME AND ADDRESS SRI International 333 Ravenswood Menlo Park, California 94025	10. PROGRAM ELEMENT, PROJECT, TASK AREA & WORK UNIT NUMBERS
11. CONTROLLING OFFICE NAME AND ADDRESS Department of the Navy Naval Air Systems Command Washington, D.C. 20361 Attn: Code AIR 33	12. REPORT DATE 23 December 1983
	13. NUMBER OF PAGES
14. MONITORING AGENCY NAME & ADDRESS(if different from Controlling Office)	15. SECURITY CLASS. (of this report) UNCLASSIFIED
	15a. DECLASSIFICATION/DOWNGRADING SCHEDULE

16. DISTRIBUTION STATEMENT (of this Report)

APPROVED FOR PUBLIC RELEASE:
DISTRIBUTION UNLIMITED

17. DISTRIBUTION STATEMENT (of the abstract entered in Block 20, if different from Report)

18. SUPPLEMENTARY NOTES

The views, opinions, and/or findings contained in this report are those of the authors and should not be construed as an official Department of the Navy position, policy, or decision unless so designated by other official documentation.

19. KEY WORDS (Continue on reverse side if necessary and identify by block number)

MICROWAVE DISCHARGE, MICROWAVE PLASMA, PLASMA CHARACTERISTICS POWER TRANSFER

20 ABSTRACT (Continue on reverse side if necessary and identify by block number)

Characteristics of gas breakdown caused by high-power microwaves were studied experimentally. This study concentrated on characterizing the breakdown plasma and on power transfer through the plasma. The integrated electron density was measured via 94 GHz interferometric technique. The decay time of visible light emission from the breakdown plasma was measured to correlate with photographic measurements of size and shape. The effect of echoes within the test chamber on pressure measurements from the discharge was investigated. The

DD FORM 1 JAN 73 1473 EDITION OF 1 NOV 65 IS OBSOLETE

UNCLASSIFIED

SECURITY CLASSIFICATION OF THIS PAGE(When Data Entered)

topic of enhanced power transfer to a reflecting metal surface, due to formation of a microwave discharge above the surface, was considered. The power transferred in the forward direction through the microwave discharge was measured using a small slit in a reflecting metal plate.

CONTENTS

ILLUSTRATIONS

ACKNOWLEDGMENT

The authors would like to express their thanks to the technical staff at SRI, especially Robert Mora and Ted Swift, who spent many hours on the experiments and equipment adjustments, and to Rebecca Moseley and Elaine Gabb for help in report preparation. We would like to thank James Willis of the Naval Air Systems Command for his help and encouragment. Mr. Willis helped coordinate our work with others studying microwave discharge phenomena.

I INTRODUCTION

Concentrated microwave energy acting on a gas can result in breakdown of the air, producing a gas discharge consisting of a dense plasma of electrons and ions. Such a discharge plasma modifies the normal tranmission of microwaves through the gas. The discharge plasma reflects some of the incident microwave energy, transmits a portion of the incident energy, and converts the energy absorbed by the plasma into pressure waves and thermal energy. Studies of possible applications of high-power microwaves require a knowledge of self-induced microwave discharge plasmas, since the discharge limits the delivered energy. Discharges must often be avoided in high-power radars or communication equipment, and often are desired to protect sensitive receivers against damage by moderate power entering antennas connected to the receivers. The Navy and other DoD agencies have examined potential applications of high-power microwave radiation.[1*]

The threshold conditions for microwave breakdown of air are fairly well understood theoretically and have been substantially verified experimentally under most conditions of interest.[2,3] However, other characteristics of discharges, such as electron density, plasma spatial and temporal growth, and microwave absorption, transmission, and reflection, are less well understood. This report presents some results on the physical characterization of the plasma itself, including microwave transmission and integrated electron density.

The experiments and calculations described in this report establish some data points and theoretical values for use in testing current theories and speculations about microwave discharges. The data and calculations presented here are part of a larger Navy program that includes related work by the Naval Research Laboratories and by various

---

*References are listed at the end of this report.

contractors. The work presented here is intended to complement those related efforts rather than duplicating them. The work presented here continues and extends some previous work on microwave discharges sponsored by the Navy within its overall program.[4]

Section II of this report briefly describes the microwave facility used for the experiments. Section III gives details of the experiments. Section IV presents the results deduced from the experimental data. Section V discusses heat transfer to surfaces adjacent to microwave discharges. Finally, Section VI summarizes the results and recommends further work.

II SRI MICROWAVE FACILITY

Figure 1 illustrates the facility. The microwave source consists of a 250-kW transmitter capable of pulse durations as long as 8 microseconds and with a maximum duty cycle of 0.001. The transmitter operates at 9.375 GHz. Microwave energy from the transmitter is concentrated into a beam via a parabolic dish and a horn feed (displaced from its normal focal position). The beam of microwave energy is directed into a vacuum vessel, where the breakdown phenomena and characteristics are studied. Microwave absorber surrounds the bell jar on the outside and can be placed inside on the bottom to minimize reflections.

The experiments described here used a metal reflecting plate placed inside the bell jar at the focal plane of the concentrated beam. The metal plate resulted in a standing wave of electric field above the plate. Microwave breakdowns occurred at one or more antinodes of the electric field (i.e., at half-wavelength intervals of 1.60 cm), beginning 0.80 cm above the plate. The 3-dB width of the focal region, transverse to the beam propagation direction, was 1.4 wavelengths. Initially, the power level and concentration efficiency resulted in a peak power flux of 1.6 kW/cm^2. This permitted breakdown with no reflecting plate present at pressures up to 20 torr, and breakdown with a reflecting plate present at pressures up to about 35 torr. The ratio of collision frequency (in the discharge) to radian radio frequency is about 2 to 3 times at these pressures and so is slightly into the collision-dominated regime of microwave discharges. During the experiments, the transmitter tube gradually failed and was eventually replaced. Some experiments were made at reduced power output, prior to the arrival of a replacement tube. The power flux was recalibrated for those experiments.

The transmission and integrated electron density experiments required modification, described later, of the basic facility.

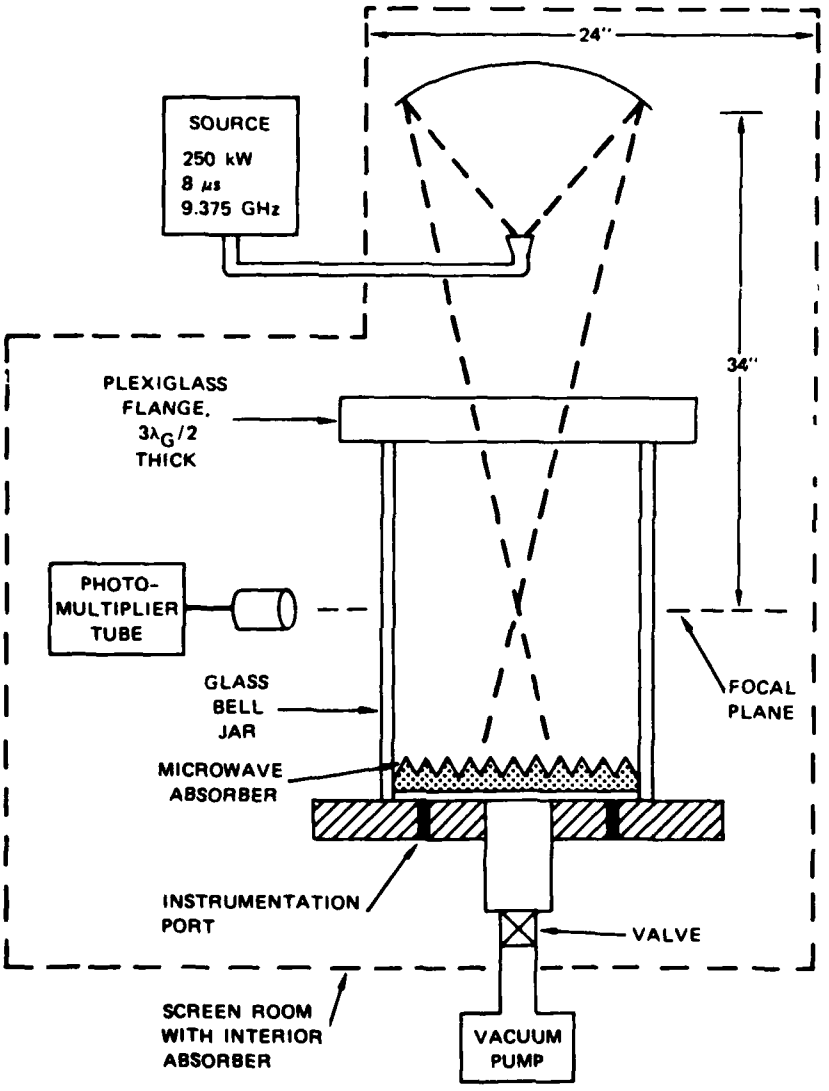

FIGURE 1 SRI MICROWAVE FACILITY TEST ARRANGEMENT

III EXPERIMENTS

A. Pressure Pulse Variation

Some pressure measurements were made to verify that measurements taken in the prior program were free of pressure echoes. Previous pressure measurements sometimes showed substantial amplitude variation from discharge to discharge.[4] Those measurements were made with a pulse repetition frequency of 10 Hz. It was suggested that the variation was caused by echoes of strong pressure disturbances inside the vacuum chamber. For example, at 30 torr, normalized overpressures of as much as 0.9 (27 torr) were obtained. The strong pressure disturbances inside the chamber might echo off the chamber walls and distort the local gas density at a breakdown region, thereby modifying (1) the time required for breakdown to occur, and (2) the net pressure produced by a subsequent breakdown.

At the request of Mr. Willis of NAVAIR, pressures produced by the discharge were measured again, but with the microwave pulse repetition rate reduced to much less than 1 pps. That pulse interval should be sufficient for any pressure echoes to be well damped. If echo caused the pressure amplitude variation, then the lower repetition rate should eliminate echoes and their associated variations.

Pressures were measured with the same apparatus used previously,[4] but with a slightly modified physical arrangement of the RF equipment. The change in arrangement caused breakdown to form secondarily at the second antinode for the electric field standing wave, as well as primarily at the first antinode. Consequently, the peak pressure wave is accompanied by a second disturbance that occurs later in time (since it travels further to the sensor). Nevertheless, if echoes are present to any significant extent, they should be similarly damped at a repetition rate of less than 1 pps. Note that a reflected wave traveling a

typical vacuum chamber dimension of 1 m at 345 m/s should echo in a few milliseconds.[5]

Figure 2 shows a typical result when the microwave pulses are well separated in time. The oscillogram has four traces. The top trace shows the RF power that produces the microwave discharges. This trace is inverted; that is, when the microwave power is on, the trace is low (at the beginning of the trace), and when the power is off, the trace returns to the baseline and is high. There are three traces at the bottom, representing three successive breakdowns. Two of the traces show a comparable peak primary amplitude, but differ significantly in the primary undershoot after the pressure pulse has been reflected off the metal plate holding the pressure sensor. The third trace shows only a small primary peak and a primary undershoot comparable to the lesser of the two peak responses. However, the third trace shows a larger peak secondary response than does either of the two traces that showed large primary peak responses.

Figure 2, and other data, continue to show significant pressure variations from discharge to discharge, for the case of a low microwave pulse repetition rate.

B. Optical Decay Time

The optical output from a microwave discharge region is a useful diagnostic tool. Spectroscopic examination of the light can reveal the gas species which are excited or ionized, and the temporal variation is an indicator of the dynamic processes that occur. The total visible light output as a function of time is a good indicator of when breakdown occurs. The decay of the visible light output is an indicator of the plasma afterglow dynamics. In previous work,[4] photographs were taken to ascertain breakdown region size and location. Because of hydrodynamic motion of the plasma (at velocities equal to or greater than 345 m/s) after the discharge forms, it is important to estimate size and location

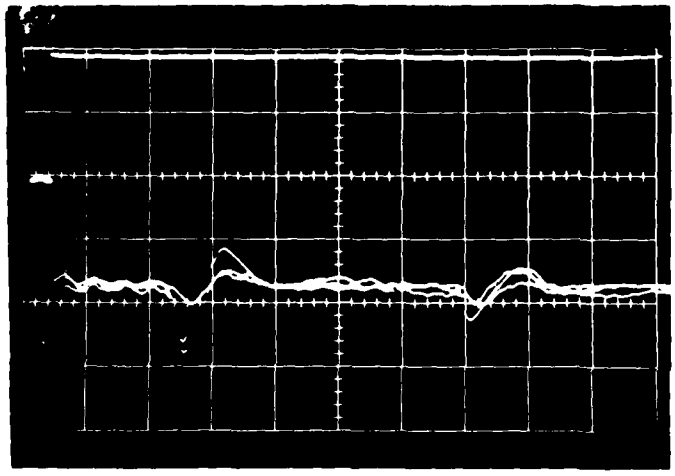

TOP TRACE — RF POWER

BOTTOM TRACES — PRESSURE SENSOR RESPONSES
(arbitrary units)

AMBIENT PRESSURE — 28 Torr
10 μs/DIV ALONG x-AXIS

FIGURE 2 PRESSURE WAVES EMANATING FROM THE MICROWAVE BREAKDOWN REGION. (The breakdowns occurred once every few seconds.)

discrepancies resulting from motion during the decay period. Accordingly, the decay time of the total light output was measured using a photomultiplier tube sensor and an oscilloscope. The visible output was found to decay quickly, in about 3 μs (at 30 torr) after RF power was turned off.

C. Power Transmission Through Discharge

The microwave power flux was recalibrated prior to measuring power transmission through the discharge region because of an observed dropoff of breakdown capability in the vacuum chamber. The power flux had fallen sufficiently so that breakdown with the reflecting metal plate could no longer be obtained above 30 torr. Alignment of the feed horn and reflector was first checked, and minor adjustments were made. However, that failed to correct the flux dropoff. The transmitter power was then measured at 130 kW, rather than its original level of 250 kW. This falloff was due to tube aging and/or modulator problems. A new tube was ordered, after no modulator problems were discovered. The power flux was recalibrated in order to continue measurements while awaiting delivery of the new tube.

The source power was measured at the transmit horn, through a series of couplers and precision attenuators. A low-power source was then substituted for the high-power source, and a receiving horn was placed approximately at the breakdown region position. The power level was measured at the transmitting horn location and at the receiving horn location, using the constant low-power source. The attenuation between the transmitting horn and the receiving horn was -13.5 dB. This attenuation resulted from several factors: losses in the focusing system, minor losses in the transmitting and receiving horns, and losses in entering the vacuum chamber through the plexiglass top. The power flux level at the breakdown region was then computed using the high-power source level at the transmitting horn, the measured attenuation between transmitting horn and receiving horn, and the calculated

effective area and pattern of the receiving horn. The peak power flux at the breakdown region is computed at 780 W/cm^2, for the 130-kW high-power transmitter level.

In addition, the power transmission measurements required an accurately calibrated video detector. A tunnel diode was used as the detector. It was calibrated over the range of interest by measuring its output as continuous-wave (CW) incident power applied to it was varied. The incident power was varied with a precision attenuator and was monitored with a power meter via a directional coupler. The tunnel detector output was found to be accurately represented by the relation $P = kV^2$ over the range of interest, where P is the power and V is the tunnel diode detector output voltage.

For this experiment, the metal reflecting plate was modified. A slit 1 mm wide and 1 cm long was cut in the center of the metal reflecting plate. Behind the plate, a section of waveguide transmitted power, coupled through the slit, to the tunnel diode detector. The slit was at the center of the focal region and was oriented so that current flow on the plate was perpendicular to the long dimension of the slit. That is, the slit lay along the H-field direction of the incident wave. The size of the slit was chosen so that power to the tunnel diode detector was below burnout of that device and was within the calibration range (up to 200 mV).

The experiment was performed by monitoring the tunnel diode output while full 130-kW power was applied at various pressures. At sufficiently high pressures, no breakdown occurred, and the tunnel diode output was constant (slight droop corresponding to transmitter sag) during the RF pulse. When breakdown occurred, the power level decreased at some time during the RF pulse. The fractional decrease in the detected power resulting from breakdown was then determined using the square-law calibration.

If the cross section of the breakdown region is sufficiently large in comparison to slit length, this method accurately measures the fractional transmission through the breakdown plasma. In most cases,

the breakdown region was a few times larger than the slit length. Therefore, the measurements are a good measure of the fractional power transmitted through the center of the breakdown region. The fractional power resulting from breakdown is due to absorption in the plasma and to reflection from the plasma. With the experimental arrangement used here, the reflection from the plasma could not be determined. Normally, the power reflected back into the transmitting horn would be measured using a directional coupler that is sensitive to reflected power.

In our experiments, the reflected power was made up largely of steady signals due to horn mismatch to free space, reflection from the plexiglass plate covering the vacuum chamber, scatter from the reflecting metal plate region surrounding the breakdown region, scatter from vacuum chamber walls, etc. In other words, the normal reflected signal swamped any signal due to plasma reflection. The fractional transmission to the slit therefore cannot be separated into parts due to absorption and reflection, using the measurements alone.

Figure 3 shows the results of this experiment, at pressures of 30, 20, 17, 15, and 10 torr. Due to the peak power flux of 780 W/cm^2 available for this experiment, breakdown was not obtained at 30 torr and above. Figures 3b through 3e show that the time for breakdown steadily diminishes as pressure is reduced, for constant power flux. Also, the transmitted power level after breakdown decreases somewhat as pressure is reduced.

Other oscillograms, not shown here, reveal that the transmitted power sometimes decreases in several abrupt steps. This was visually correlated on several occasions with the occurrence of multiple breakdown regions. At other times, there is only a single large step decrease in transmitted power, even through several breakdown regions are present. Thus, it appears that sometimes breakdowns in the extra regions occur sequentially in time with separations of a few hundred manoseconds, while at other times breakdown in all the regions occurs nearly simultaneously.

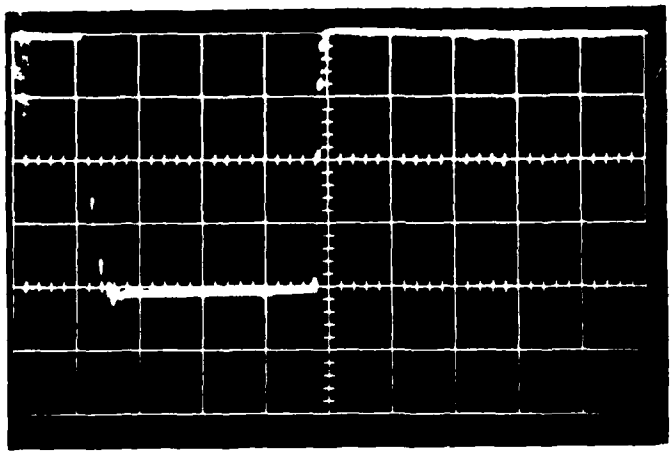

(a) 30 torr,
NO DISCHARGE

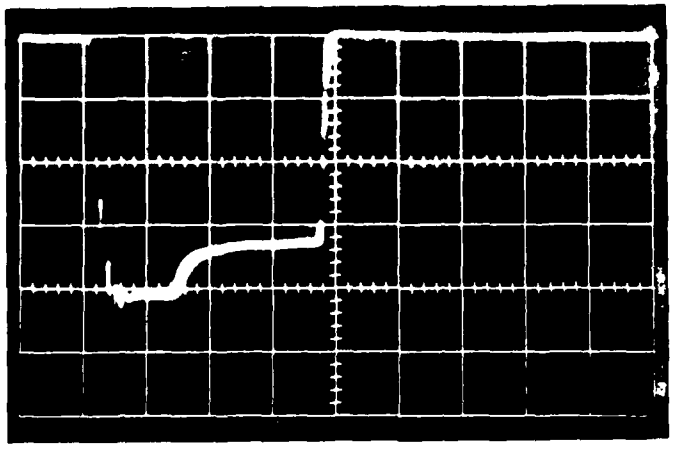

(b) 20 torr,
DISCHARGE

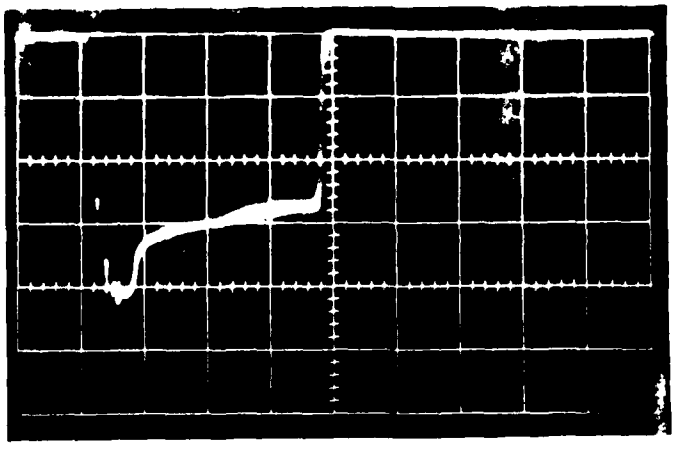

(c) 17 torr,
DISCHARGE

FIGURE 3 TRANSMISSION THROUGH MICROWAVE DISCHARGE INTO A SLIT IN A REFLECTING PLATE (S = 780 W/cm^2, 10 pps, 1 μs/division horizontal, 0.05 V/division vertical)

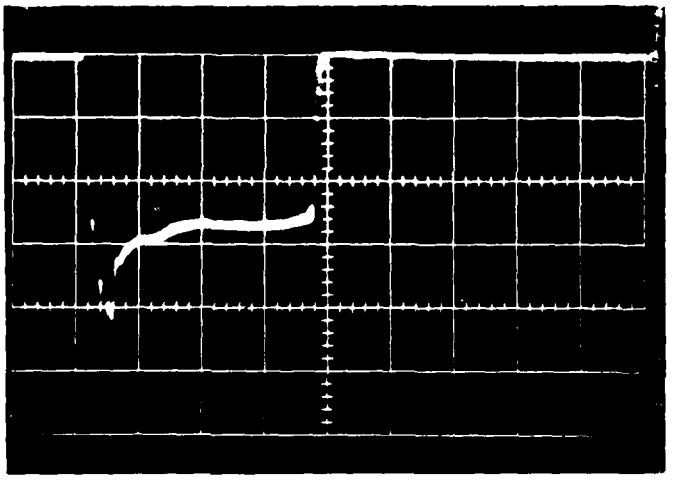

(d) 15 torr, DISCHARGE

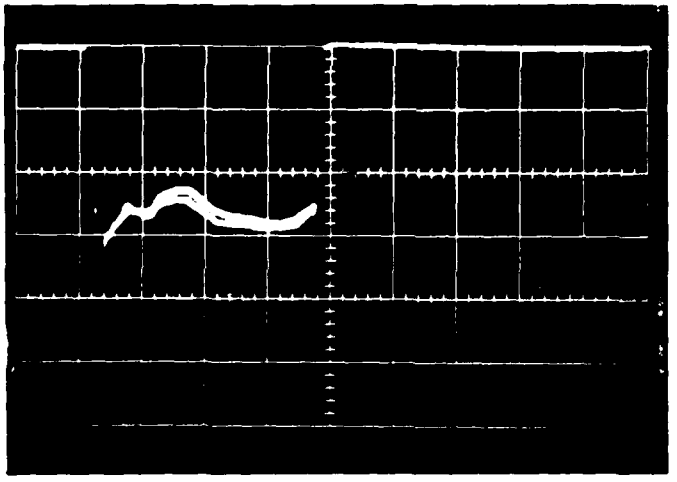

(e) 10 torr, DISCHARGE

FIGURE 3 (Concluded)

D. Integrated Electron Density

A microwave interferometer was set up to measure the integrated electron density of the discharge region. In a previous program,[4] the ion density was measured within the breakdown plasma using Langmuir probes. The integrated density was then estimated, using data from a separate (optical) thickness measurement. However, Langmuir probes interfere with plasma formation and may have contaminated those measurements. In addition, since the breakdown plasma forms in multiple regions, it is difficult to estimate integrated electron density from a single probe measurement. Multiple probes used to profile the discharge region would result in substantial interference. In addition, the optical thickness measurement has some inaccuracies due to motion during the exposure time. Consequently, it was important to try to measure the integrated electron density of the breakdown region and thereby validate the previous individual measurements of peak electron density and breakdown region thickness.

The electron density and size of the discharge region in our experiments were such that it was difficult to make point or integrated electron density measurements using optical techniques, without resorting to extreme power levels that might directly affect the breakdown process. Consequently, microwave interferometry was judged to be the most suitable technique for measuring integrated electron density. Interferometry is noncontacting, and therefore noninterfering, when low power levels are used. Microwave interferometry is also fairly sensitive to low levels of electron density and of integrated electron density. The main disadvantage of microwave interferometry is that it measures only integrated electron density and not point density. In some cases, point density can be deduced by profiling a plasma region. However, the profiling resolution is limited by the size of the microwave interferometer beam--typically a few square wavelengths at the interferometer frequency or larger.

The microwave interferometer used here was unusual in that the test and reference arms were the same. The interferometry was carried out by

comparing the signal when the test object (the breakdown plasma) is temporarily introduced into the test signal path, with the same signal when the test object is not present.

A 94-GHz interferometer was set up, as is illustrated in Figure 4, to measure the integrated electron density. The final arrangement is illustrated in Figure 4. Because the thickness of the primary breakdown region was only 2 mm, compared to a 3-mm wavelength at 94 GHZ, edge (end-on) illumination of the primary breakdown region was not possible; the beam was thicker than the plasma region. Initially, the 94-GHz interferometer was set up to propagate at an angle of about 45^{o} through the primary breakdown plasma located about 8 mm above the metal reflecting ground plane. However, the temporal irregularity of the primary breakdown region (sometimes it did not exist) as well as difficulties in ensuring that the 94-GHz beam passed through the primary breakdown region and not merely through its edge, led to abandonment of that arrangement. The final arrangement used a vertical path for the 94-GHz beam, so that it passed through all of the discharge regions and not through just the primary (lowest) one.

The 94-GHz source was a 200 mW Impatt. The distances involved and the low power level available required that horns be used in both the transmit and receive arms to achieve adequate signal levels. The transmit horn was located below the metal reflecting plate used to generate a standing wave for the X-band field. The horn aperture was flush with the reflecting plate. The 94-GHz horn polarization was orthogonal to the X-band polarization to minimize distortions of the breakdown region. The 94-GHz receive horn was located within the converging X-band beam and therefore scattered some X-band power and distorted the shape of the breakdown region, resulting in an elongated (rather than circular) breakdown region. This effect was minimized by locating the 94-GHz receive horn and connecting waveguide in line with, and just below, the X-band feed horn and arm, so that the 94-GHz equipment was shadowed by the X-band equipment.

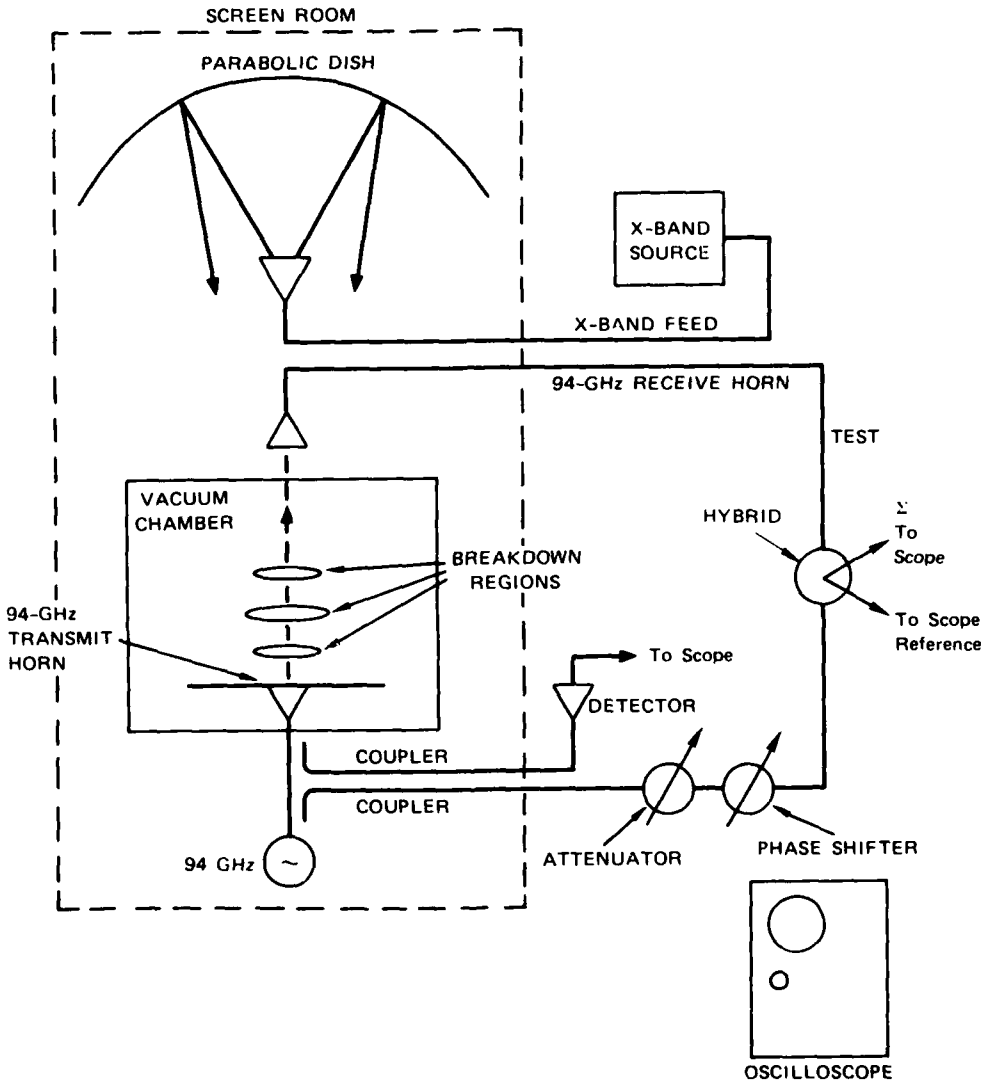

FIGURE 4 94-GHz INTERFEROMETER

Part of the 94-GHz power is split off by a 10-dB coupler before it passes through the transmit horn. This portion goes through a variable attenuator and a phase shifter before it arrives at the reference arm of a hybird circuit. The transmitted signal passes through the vacuum vessel, and through any discharge region that may be present, before it is collected by the receive horn. The received signal is then routed to the test arm of the hybird. The hybrid outputs are sum and difference signals, provided the variable attenuator and phase shifter are properly adjusted. When no breakdown plasma is present, the variable attenuator and phase shifter are adjusted to produce a maximum at the sum arm of the hybrid, and a null at the difference arm of the hybrid. When a plasma is present, the sum and difference arms become unbalanced, and their output indicates the amplitude change and phase change encountered in passing through the X-band-induced microwave discharge.

Considerable difficulty was encountered in implementing this experimental arrangement. The 250-kW X-band power is about 60 dB higher than the 94-GHz source power and about 90 dB larger than the 94-GHz signal levels at the test and reference ports of the hybrid. As a result, the X-band pulse power resulted in disturbances of the hybrid output; presumably, this was due to coupling of X-band power into the 94-GHz detector crystals. This coupling was probably due to the leakage of X-band power into the cables connecting those crystals to the oscilloscope. The hybrid circuit and the detection crystals were shielded and relocated several times and were finally placed outside the screen room. This necessitated long runs of waveguide, which further reduced signal levels at the hybrid input and output arms.

Figure 5 shows the output of the difference arm as a function of time for pressures of 3, 10, 15, 18, and 20 torr, respectively. With the interferometer in place, no breakdown occurred at or above 20 torr (due to field scattering and distortion by the 94-GHz interferometer apparatus). Therefore, the 20 torr results can be taken as the baseline case illustrating the normal level of X-band interference.

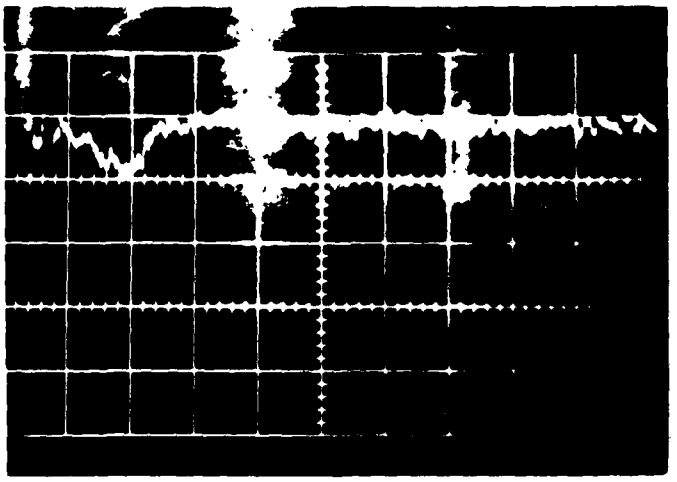

(a) 3 torr, DISCHARGE

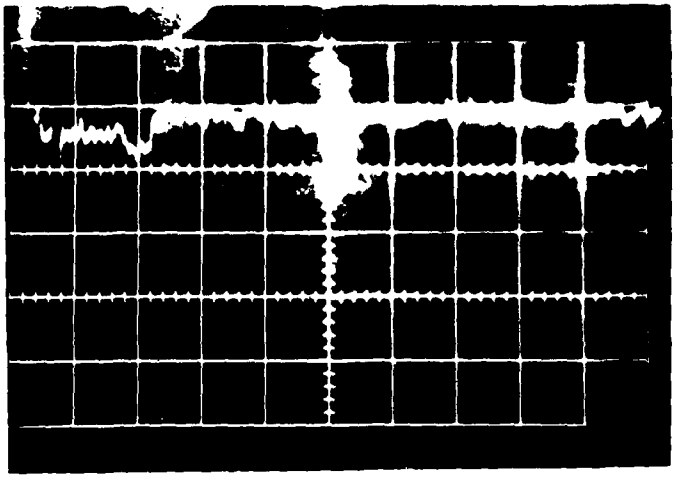

(b) 10 torr, DISCHARGE

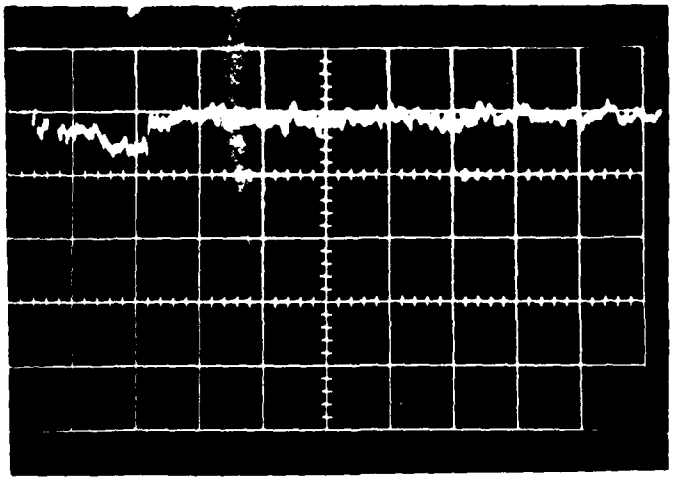

(c) 15 torr, DISCHARGE

FIGURE 5 94-GHz INTERFEROMETER DIFFERENCE ARM OUTPUT (S = 1600 W/cm^2, 10 pps, 5 μs/division horizontal, 50 μV/division vertical)

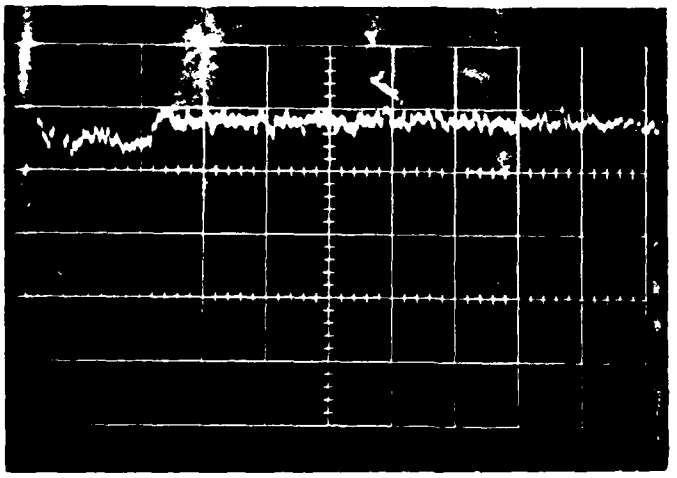

(d) 18 torr,
DISCHARGE

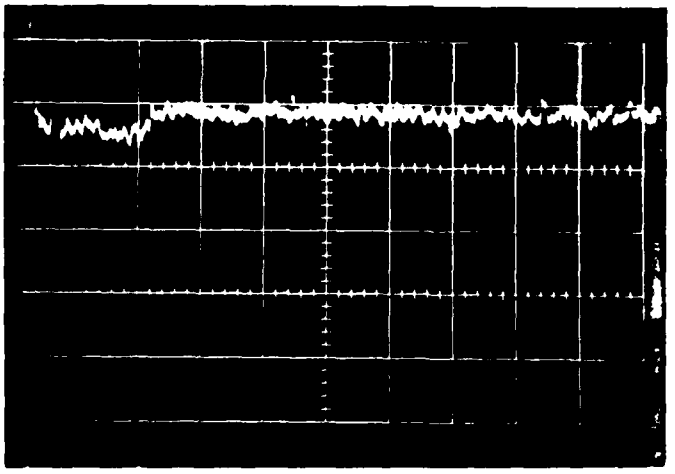

(e) 20 torr,
NO DISCHARGE

FIGURE 5 (Concluded)

For small attenuations, the sum signal is not very sensitive to changes in attenuation or phase shift, while the difference signal is sensitive primarily to changes in attenuation and phase shift. For the experimental parameters involved, it can be shown that the change in difference signal is primarily due to the phase shift term, which is proportional to the integrated electron density.

Measurements also were made of attenuation of the signal passing through the plasma. These measurements suffered from excessive X-band interference, and were difficult to interpret. The direct attenuation measurement offers another means of deriving the integrated electron density, but also includes an extra collisional term. Figure 6 shows attenuation data at various pressures.

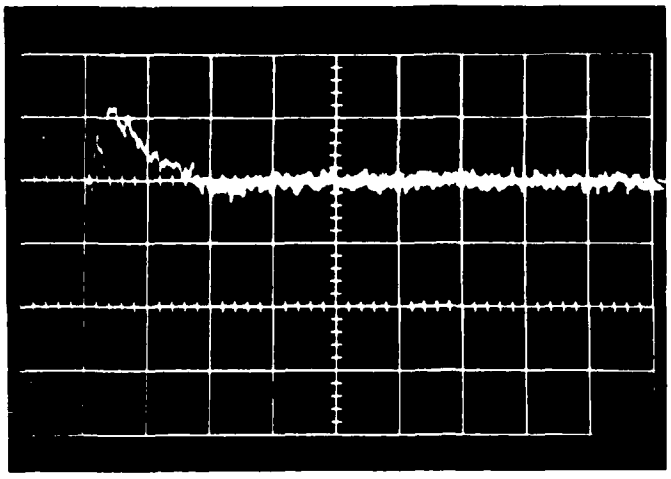

(a) 20 torr,
NO DISCHARGE

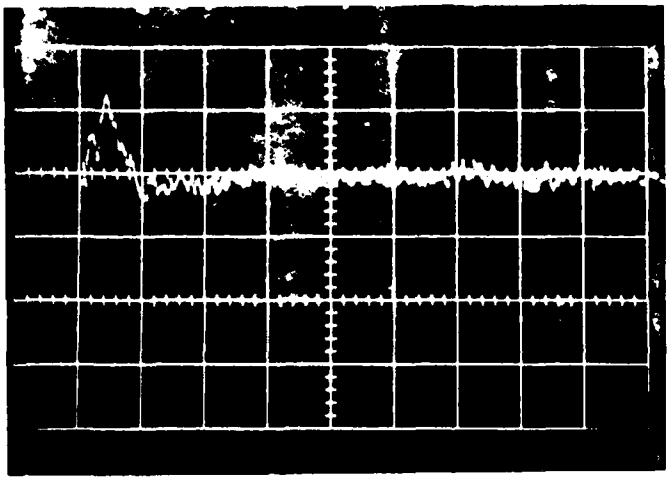

(b) 15 torr,
DISCHARGE

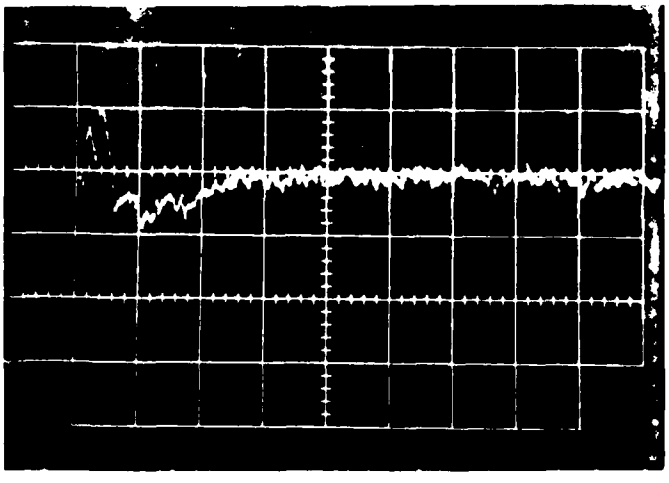

(c) 10 torr,
DISCHARGE

FIGURE 6 94-GHz ATTENUATION PASSING THROUGH MICROWAVE DISCHARGE
(S = 1600 W/cm^2, 10 pps, 5 μs/division horizontal, 50 μV/division vertical)

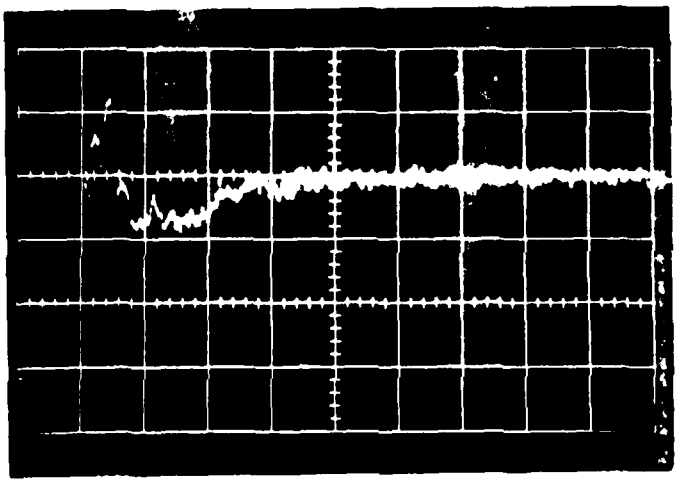

(d) 5 torr, DISCHARGE

FIGURE 6 (Concluded)

IV RESULTS

A. Pressure Pulse Variation

The slow repetition rates did not result in less variation of pressure pulses. Thus, the variation cannot be ascribed to echoes alone. However, it is still possible that echoes play some role.

The pressure pulse data were subsequently reviewed. A number of instances occur where there is little variation from shot to shot, while in other cases there is considerable variation from shot to shot. The data tend to have less variation at lower pressures than at higher pressures. This might be expected, since high-pressure measurements were made close to the threshold for breakdown, and threshold will always involve some statistical variations from the norm. The data also show a trend to more variation when multiple breakdown regions are present. Apparently, some of the regions rob power from other regions, leading to considerable fluctuations in the primary pressure pulse (the one measured most often).

Another explanation for the variation may involve the pressure sensor itself. The sensor was designed to operate primarily at high pressures, up to 3000 psi, rather than at the low end of the scale used in our experiments--about 0.6 psi or less. While the sensor nominally has resolution to about 0.05 psi, it may not reset properly to zero following small pressure disturbances. The variations may result from a residual bias following a previous sensor displacement.

The existing data and speculations about sources of the observed variations in pressure pulses from microwave discharges do not conclusively point to any single cause.

B. Optical Decay Time

The optical decay time was measured at about 3 microseconds at 30 torr. That time should vary inversely with pressure. If the discharge region is moving at the velocity of sound (345 m/s), then it will travel about 1 mm during the optical decay time. Hence, photographic measurements with still cameras could have position uncertainties of 1 mm. Likewise, photographic measurements of thickness could be off by similar amounts, if hydrodynamic motion takes place during the recording period. In previous work, the location of the primary discharge region was found to be 9.7 mm above the plate and to have a thickness of 1.9 mm.[4] Thus, it is quite possible that the thickness of the breakdown region has been overestimated. Photographs made with a framing camera could help resolve this question, because of the short exposure time.

C. Power Transmission Through Discharge

Figure 7 shows the normalized power transmitted through the discharge after breakdown occurs. Although there is a variation of transmitted power with time during the breakdown phase, the power value plotted is the minimum value observed. For example at 20 torr, the minimum fractional transmission is 65% after breakdown, while at 15 torr, the minimum fractional transmission is 40%.

The values given in Figure 7 indicate that more power is transmitted at higher pressures than at lower pressures. That may occur for several reasons. First, at lower pressures, the plasma is more diffuse, and consequently it may shield more of the entire reflecting plate, reducing coupling through the slit aperture. It was pointed out in Section III that the breakdown region is not much greater than the slit length, at least near the breakdown threshold. Second, as pressure is decreased, the plasma generally becomes a better match for the incident power, since the ratio of collision frequency to radian

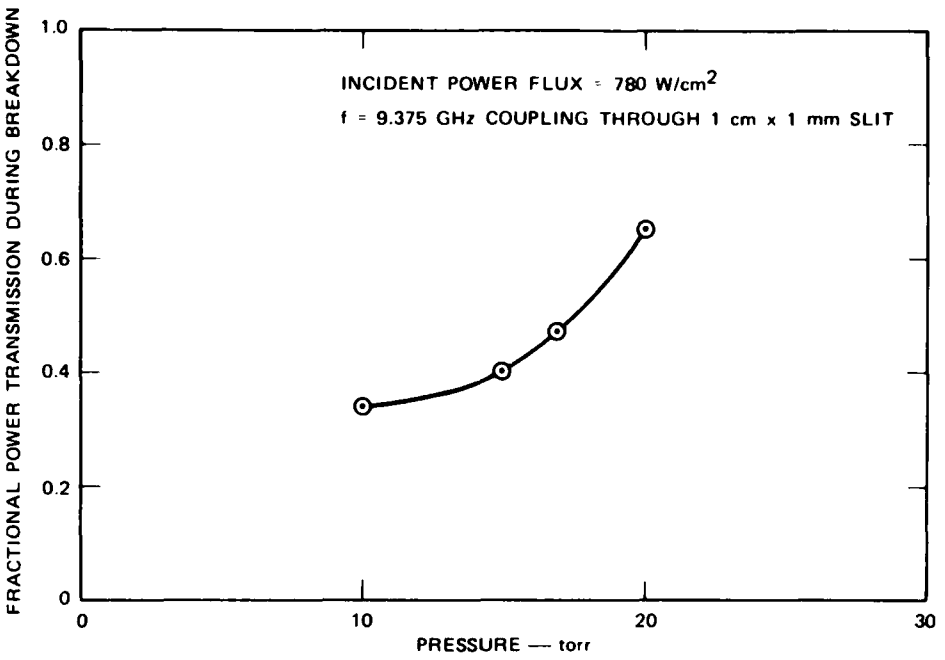

FIGURE 7 FRACTIONAL POWER TRANSMISSION DURING BREAKDOWN
(lowest transmitted power during breakdown)

operating frequency is equal to 1 at about 12 torr. Near that pressure, the constant incident flux achieves its greatest overstress with respect to the breakdown threshold, and strongest absorption should occur.

In previous work,[4] it was estimated that the fractional absorption of the breakdown plasma was 65% to 95% at 30 torr, with a power flux of 1600 W/cm^2. That would indicate a maximum fractional transmission of about 35%, a result that does not seem consistent with the values reported here. Unfortunately, equipment degradation prevented transmission experiments at conditions corresponding to the the previous investigation. Some earlier results by Scharfman[5] indicated that as power was increased, the fractional transmission through a free-space breakdown region decreased in such a way as to maintain about the same absolute transmission level. A similar phenomena might occur here, but data with that parametric variation were not gathered.

D. Integrated Electron Density

Figure 8 gives the integrated electron density derived from the 94-GHz measurements as a function of pressure, at constant fixed power flux (1600 W/cm^2). The integrated electron density decreases with pressure by a slight amount. In general, the integrated electron density measurements cover multiple breakdown regions, so that little can be said about peak density, even for a single breakdown region. Figure 8 also shows a speculative maximum value of integrated electron density equal to $10^{14}/cm^2$ multiplied by the ambient pressure in atmospheres, valid for the high pressure regime. That speculative value is based on near-total absorption of the incident high-power microwave field. Actually, however, if the ionization front moves rapidly, then the speculative value could be exceeded, because only the active absorbing volume need conform to the above limit, and a low-density, large-integrated-density tail could exist behind the moving ionization front. For the low pressure regime, the integrated electron density is expected to be limited to the product of the critical density ($1.1 \times 10^{12}/cm^3$) and about one-half wavelength of path. The measured integrated electron density poorly matches the speculative value, but is close to the expected low presure value.

The integrated electron density at peak power flux and 15 torr pressure compares reasonably well with the $1.0 \times 10^{12}/cm^2$ value estimated in earlier work based on estimated thickness and on estimated peak electron density. The discrepancy is believed to be due to the two estimates, as well as to the disturbance of electric fields in the breakdown region engendered by the 94-GHz interferometer apparatus. The disturbance of the breakdown region due to scattering from the 94-GHz apparatus can be minimized by going to higher 94 GHz powers, which would then permit the use of smaller horns.

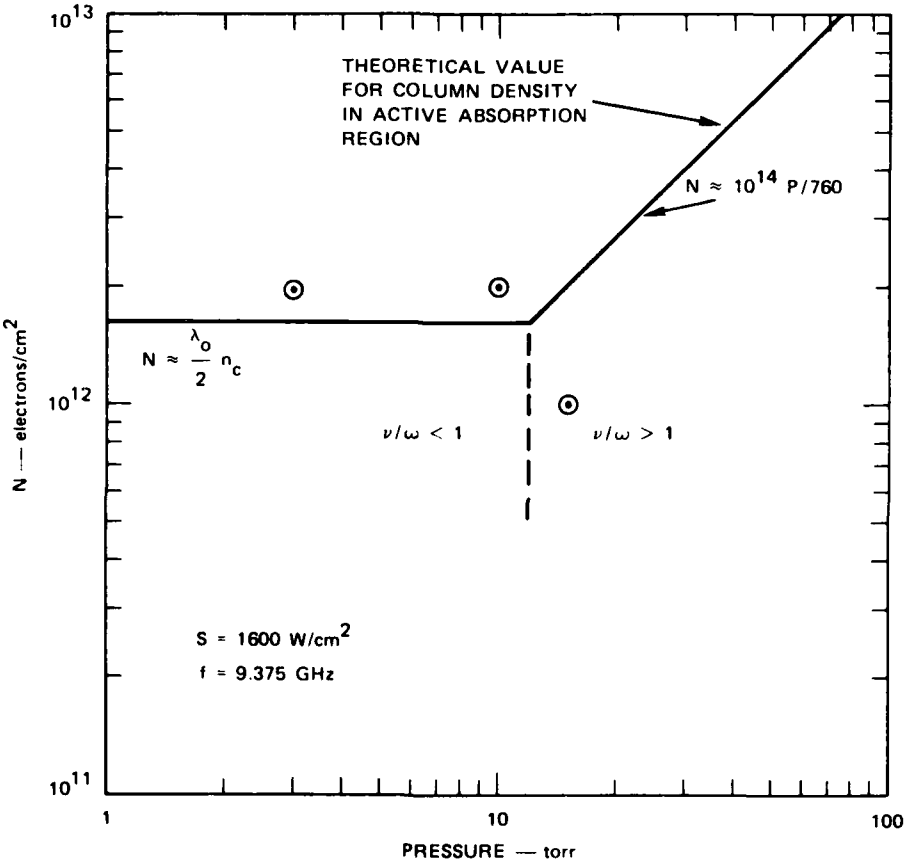

FIGURE 8 INTEGRATED ELECTRON DENSITY

V THERMAL TRANSFER CONSIDERATIONS

Microwave energy incident upon a metal surface of high conductivity is largely reflected, and very little energy is converted into heat. For example, at normal incidence, the fraction of the incident energy, or power flux, converted to heat is

$$F = \frac{2}{3}\sqrt{\frac{f\mu_r}{\sigma}} \quad ,$$

where f frequency in GHz

μ_r Relative permeability of the metal

σ Conductivity of the metal, mhos/m.

For copper at 10 GHz, $F = 2.77 \times 10^{-4}$, i.e., 0.03%.

The temperature rise of a slab of the conducting material is readily calculated for a given incident power flux and pulse duration, provided (1) the thickness of the material is known, (2) the specific heat is known as a function of temperature, and (3) losses due to conduction, convection, and radiation are included. Assuming adiabatic conditions (ignoring conduction, convection, and radiation), a copper film of thickness 1 mil (2.5×10^{-3} cm), and a constant specific heat, then the temperature rise is

$$\Delta T = 0.032\ St$$

where S is in W/cm^2, t is in seconds, and ΔT is in degrees Centigrade.

For the SRI experimental apparatus, with $S = 1600\ W/cm^2$ and $t = 8\ \mu s$, $\Delta T = 0.0004^{o}C$. That value is not measurable with our equipment, for a single pulse. Over a 1-s period, with a maximum repetition rate

allowed by the transmitter duty cycle (125 pps), the temperature rise is only 0.05°C. In reality, operation at pressures of interest (5 to 30 torr), and with real support structures for the thin film, would result in a much smaller temperature rise.

It has been speculated that causing a microwave discharge to form near the surface of a highly conducting body will greatly enhance heating of that body, due to heat transported from the discharge. Enhancement of body heating due to microwave discharges was to be investigated, time permitting. However, the other investigations reported here took longer than anticipated, and precluded experimental examination of the enhancement. Also, enhancement was being investigated experimentally at the same time by T. Whiting of the Naval Research Laboratories in a related program. Therefore, only selected considerations regarding enhanced energy transfer in the presence of a discharge plasma were examined.

Previous work indicated that the breakdown plasma created near a surface could absorb nearly all the microwave energy incident upon the body. However, as has been observed in experiments at SRI and elsewhere, the breakdown region tends to spread away from the body, whenever that is possible for the total field configuration (composed of the incident microwave beam and the scattering from the body). This spreading implies that the incident microwave energy will be absorbed in a volume equal to the body-projected cross section multiplied by a large number of wavelengths (say 10 for generality). The breakdown region will gradually heat up, and eventually, hydrodynamic behavior will take place. The heated region will flow both toward the target, where much of the flow will be reflected, and away from the breakdown region toward the source. A microwave-supported-combustion or -detonation wave will occur. The body will be heated by some of the mass flow toward it, and by some of the radiated heat from the breakdown region. Assuming the discharge absorbs 100% of the incident energy, no more than 50% can be directed toward the body. The dimensions of the breakdown region limit the time for hydrodynamic flow, and therefore limit gas heating within

the active absorption region. Typically this dimension is a small portion of a wavelength, say 1/8. In a one-dimensional flow situation, the maximum heat flux toward the target within this time would be

$$Q = \frac{St}{2}$$

where $t = \frac{d}{v} \approx \frac{\lambda}{8v}$

$v = 34500$ cm/sec

At 10 GHz, t = 1.1 microsecond, and Q = 8.7×10^{-4} joules/cm^2 for S = 1600 w/cm^2. This energy input would raise the film temperature by about 42^{o}. Heat deposited in the gas volume would reduce this value. Reflection of flow would further reduce this value. For longer times, lowered heat input would provide a more gradual increase in temperature.

The considerations here indicate that measureable temperature rises may occur when a discharge plasma forms over a thin metal reflecting plate.

VI SUMMARY

Some experiments were performed in the SRI microwave facility to help characterize the physical properties of gas discharges caused by high-power microwaves. The experiments measured (1) the power transmitted through a discharge above a coupling slit in a ground plane, and (2) the integrated electron density above a reflecting ground plane. Some auxiliary measurements were made to ascertain whether echoes caused some observed variations in pressure pulses from microwave discharges and to determine the optical decay time constant associated with prior photographic measurements of discharge size and location. Enhanced thermal heating of metal surfaces due to nearby microwave discharges also was considered. This section summarizes the measurements, the results deduced from them, and the supporting calculations.

The microwave power flux incident on the discharge region was 1.6 kW/cm^2 for the integrated electron density measurements and pressure pulse variation mesurements, and 0.78 kW/cm^2 for the coupling measurements. Pulses were used with durations of 4 to 8 μs at repetition frequencies of 10 pps or slower. These pulses created discharges in regions about 1 cm above the reflecting plate in the vacuum chamber, and at additional antinodes spaced about 1.6 cm apart. Experiments were generally conducted between a few torr and 40 torr. Microwave discharges usually occurred at pressures between 20 to 35 torr, depending on the specific experiment.

The echo experiments showed that pressure pulse variations were not attributable to echoes bouncing off chamber walls and disturbing air density within the vacuum chamber. Possible causes of the variations are: statistical deviations of the breakdown process, especially near breakdown threshold at higher pressures; multiplicity of discharge

regions with irregular power division between them; and the resetting capability of the pressure sensor itself.

The optical decay time of light from the discharge was measured at about 3 μs. Taken together with the possible speed of hydrodynamic expansion, the thickness of the plasma estimated from photographs may be in error by 1 mm. That is a significant error compared to the original 2-mm estimated thickness.

Power transmitted through the discharge to a slit in the reflecting plate was found to decrease as pressure decreased, and ranged from 65% at 20 torr to 34% at 10 torr. This indicated less absorption than was expected from higher-pressure measurements.

The integrated electron density was measured using an interferometer arrangement at 94 GHz. The measurements gave an integrated density of 1 to 2 x 10^{12} electrons/cm^2, depending on pressure. That measurement is not highly accurate because breakdown only slightly unbalanced the interferometer bridge output.

Enhancement of surface heating, due to a discharge forming over a reflecting metal surface, was briefly considered. Provided the surface is a thin film, significant temperature rises appear possible. Lack of time precluded experimental verification of this possibility.

Recommendations to improve and/or extend the data base on characteristics of microwave discharges are as follows:

(1) Measure pressure pulses produced by microwave discharges at higher pressures.

(2) Measure spatial properties of microwave discharges using framing camera techniques.

(3) Measure near-backscatter and side-scatter from microwave discharges, using a larger experimental facility allowing reduced instrument perturbations.

(4) Measure temperature rises of thin reflecting films near microwave discharges.

REFERENCES

1. J. J. Gallagher, H. A. Ecker, M. D. Blue, and R. G. Shackelford, "Applications of Submillimeter Wave Gigawatt Sources," Final Report, Office of Naval Research Contract N00014-75-C-1011, Georgia Institute of Technology, Atlanta, Georgia (1975)

2. W. C. Taylor, W. E. Scharfman, and T. Morita, "Voltage Breakdown of Microwave Antennas," Advances in Microwaves, Vol, 17 (Academic Press, Inc., New York, 1971).

3. A. D. McDonald, Microwave Breakdown in Gases (John Wiley and Sons, New York, 1966).

4. S. A. Damron and G. August, "Physical Constants for Microwave Discharges in Air," Final Report, Naval Air Systems Command, Contract N00019-81-C-0479, SRI Project 3681, SRI International, Menlo Park, California (October 1982).

5. W. E. Scharfman, W. C. Taylor, and T. Morita, "Research Study of Microwave Breakdown of Air at High Altitudes," Final Report, AFCRL-62-732, Air Force Cambridge Research Laboratories, Contract AF 19(604)-7367, SRI Project 3345, SRI International, Menlo Park, California (August 1962).

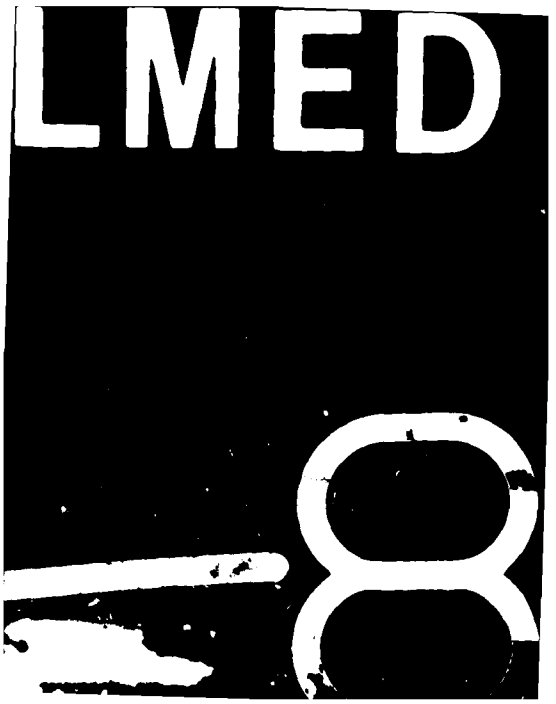
LMED